

<sup>5</sup>We use the notation  $\eta_{\alpha\beta} = (-C^{-1})_{\alpha\beta}$  where  $C$  is the charge conjugation matrix. For Majorana spinors  $\bar{\theta}_\alpha \equiv (\theta^\dagger \gamma^0)_\alpha = \theta^\beta \eta_{\beta\alpha}$ . The choice  $\Gamma^\mu = \gamma^\mu$  corresponds to the global supersymmetry of Ref. 1.

<sup>6</sup> $\epsilon_{\alpha\alpha'}$  is the real antisymmetric charge matrix in the  $O(2)$  internal-symmetry space:  $\epsilon_{12} = 1 = -\epsilon_{21}$ . The contribution to  $h_{\mu\alpha}(z)$  which is independent of  $\theta^\alpha$ , i.e.,  $\bar{\psi}_{\mu\alpha}(x)$ , has been omitted in Eq. (3) as it is pure gauge and can be eliminated by the gauge transformation  $\xi^\mu = \bar{\lambda}^\mu(x)\theta$ ,  $\xi^\alpha = 0$ .

<sup>7</sup>As pointed out recently by S. Weinberg (to be published), it is the *formal* scale invariance of certain global supersymmetric models that prevents the breakdown of supersymmetry at the dynamical (loop) level. (The scale anomalies apparently do not modify this result.) Thus the appearance of explicit breakdown of scale invariance in gauge supersymmetry implies that the further dynamical breakdown of the remaining global supersymmetry is to be expected.

<sup>8</sup>As pointed out by R. Jackiw [in *Laws of Hadronic*

*Matter*, International School of Subnuclear Physics "Ettore Majorana," Erice, 1973, edited by A. Zichichi (Academic, New York, 1975), p. 225], the breakdown of scale invariance should lead to a Goldstone boson whose subsequent Higgs absorption might result in a mass growth for the graviton. Such a mass growth does indeed occur here, but for  $p_{\mu\nu}$  and not  $g_{\mu\nu}(x)$ , and so the graviton remains correctly massless.  $\varphi_0$  and  $S_\mu$  in Eq. (3) are the Goldstone bosons absorbed by  $p_{\mu\nu}$ .

<sup>9</sup>One has  $\mu_r = \frac{1}{2}[\epsilon, \epsilon\tau_1, i\tau_2, \epsilon\tau_3]$ , where  $[\mu_r, \mu_s] = -\epsilon_{rst}\mu_t$ . <sup>10</sup> $\Gamma_+$  and  $\Gamma_-$  differ only by chiral interchange. Spontaneous breaking, of course, can only say that the theory prefers one chiral state over the other, but not which one.

<sup>11</sup>The chiral right mesons also grow additional masses by this mechanism.

<sup>12</sup>There is also a second massless vector meson in the  $U(2) \otimes U(2)$  set corresponding to heavy-particle number (or lepton number). There exists the possibility that this meson acquires a mass dynamically.

## Fusion of $^{14}\text{N} + ^{12}\text{C}$ at Energies up to 178 MeV\*

R. G. Stokstad, J. Gomez del Campo,† J. A. Biggerstaff, A. H. Snell, and P. H. Stelson  
Oak Ridge National Laboratory, Oak Ridge, Tennessee 37830

(Received 5 April 1976)

The cross section for the fusion of  $^{14}\text{N} + ^{12}\text{C}$  has been determined at bombarding energies covering the range  $E_{^{14}\text{N}} = 43\text{--}178$  MeV (3 to 12 times the interaction barrier height). The cross section decreases slowly with increasing energy and, at the highest energy, suggests that  $^{26}\text{Al}$  has been formed with an angular momentum equal to the liquid-drop limit.

Although there is considerable experimental information on fusion cross sections,  $\sigma_{\text{fus}}$ , for heavier systems,<sup>1</sup>  $A_1 + A_2 \gtrsim 40$ , little information is available at high energies for lighter systems with  $A_1 + A_2 \lesssim 30$ . This may be due to the serious difficulty of separating the products of direct inelastic reactions and of fusion when the evaporation residues have masses comparable to or less than that of the projectile. Experimental information in this mass region is especially desirable because of the microscopic,<sup>2</sup> time-dependent Hartree-Fock<sup>3</sup> calculations which are now becoming available for reactions involving light targets and projectiles. We have therefore undertaken to measure the reaction products for the system  $^{14}\text{N} + ^{12}\text{C}$  for a wide range of incident energies. An important contribution to our ability to deduce fusion cross sections from these measurements has been the development of a Hauser-Feshbach computer code<sup>4</sup> which predicts the laboratory energies, angular distributions, and relative intensities of the evaporation residues. The main re-

sult of our measurements is that  $\sigma_{\text{fus}}$  decreases slowly over an energy range extending from about 3 times to 12 times the interaction barrier; at the highest energy the deduced critical angular momentum equals the limit predicted for a rotating liquid drop.<sup>5</sup>

Beams of  $^{14}\text{N}$  produced by the Oak Ridge isochronous cyclotron at seven energies in the range 43.9 to 178.1 MeV were used to bombard carbon foils of 156 and 257  $\mu\text{g}/\text{cm}^2$ . The target thickness was determined by weighing the foils and by Rutherford scattering at 19 MeV. The two methods agreed within their errors of  $\sim 4\%$  and  $\sim 6\%$ , respectively. The principal contaminants in the target were  $^{13}\text{C}$  (1%),  $^{16}\text{O}$  (1.3%), and hydrogen ( $\approx 2\%$ ). Reaction products with  $Z = 3$  to 12 were identified with a  $\Delta E$  (ionization-chamber)- $E$  counter telescope. Angular distributions were measured in the range  $4^\circ$  to  $40^\circ$  (lab). The accuracy of the absolute normalization is estimated to be about  $\pm 8\%$ .

The yields of neon, sodium, and magnesium

nuclei are clearly the residues of compound-nucleus formation followed by evaporation of light particles. These residues have a velocity distribution centered about the velocity of the compound nucleus and broadened by the recoil imparted by light-particle emission. The total yields of lighter elements, however, contain contributions from two-body reactions in which one or more nucleons are transferred. These contributions have a velocity distribution characteristic of that of the projectile, and thus have an energy typically higher than that of an evaporation residue of the same mass. They represent the portion of the total reaction cross section which is not fusion and will be discussed in a separate article.

The analysis of the reaction products relies on the knowledge that the energy distributions of the evaporation residues change in a consistent way from element to element. As the  $Z$  of the residue decreases, the average energy decreases and the width of the distribution increases. These considerations are quantified in a Monte-Carlo statistical-model code<sup>4</sup> which has, as an essential and previously unavailable feature, an accurate treatment of angular momentum in both entrance and exit channels. We emphasize, however, that our analysis of the reaction products is not directly dependent on this model; the calculations serve mainly to give confidence that the peak shapes assumed in the analyses of the energy spectra correspond to those expected for evaporation residues. This is illustrated in Fig. 1(a) which shows measured energy spectra of sodium and nitrogen nuclei produced at bombarding energies of 86.3 and 167.1 MeV, respectively. The histograms are the calculated spectra for evaporation residues. A comparison of measured and predicted relative yields of evaporation residues at two energies is shown in Fig. 1(b).

Before discussing the experimental results, two comments are necessary. (a) The agreement between the predicted and observed properties of the evaporation residues indicates that the yields are consistent with the formation of a compound nucleus in statistical equilibrium. Measurements and analyses of  $^{12}\text{C} + ^{14}\text{N}$  fusion products at low energies and of primary emission of particles such as  $^6, ^7\text{Li}$  and  $^7, ^9\text{Be}$  also suggest<sup>6</sup> that an equilibrated compound nucleus is formed, at least for  $^{14}\text{N}$  energies up to  $\sim 86$  MeV. (b) We have considered whether processes analogous to deeply inelastic scattering<sup>7</sup> might produce significant contributions to the yields which we identify

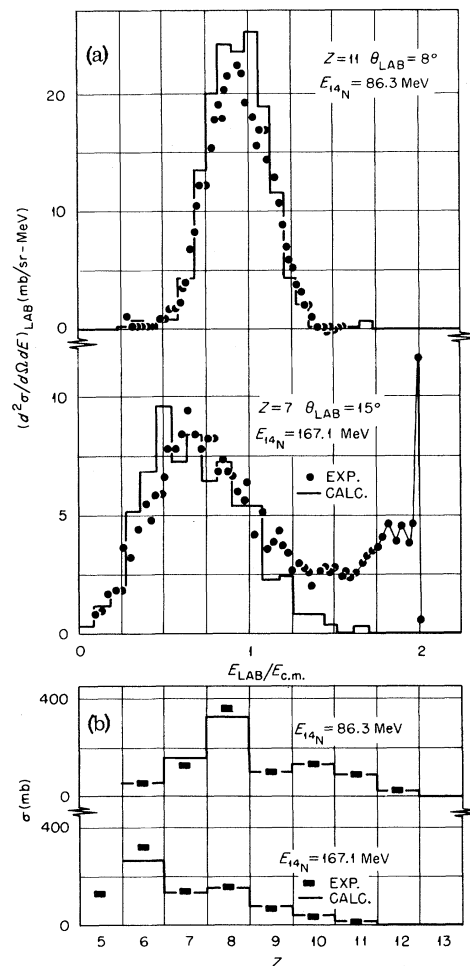


FIG. 1. (a) Energy spectra of sodium ions and nitrogen ions produced at bombarding energies of 86.3 and 167.1 MeV, respectively. The histogram is the calculated spectrum of evaporation residues normalized to the total fusion cross section. (b) Yields of evaporation residues at bombarding energies of 86.3 and 167.1 MeV. The histogram is the result of a statistical-model calculation, normalized at each energy to  $\sigma_{\text{fus}}$  and using a value of  $J_c$  consistent with the data.

as evaporation residues. If one makes the reasonable assumption that the deeply inelastic process should excite the target or the projectile with approximately equal likelihood considering their nearly equal masses, then one would expect to observe nearly equal intensities of the unexcited partners for the "deep-inelastic" yields of  $Z=6$  and  $Z=7$ . Rather than this equality, we observe that the relative evaporation residue yields for  $Z=6$  and  $Z=7$  (and other values of  $Z$  also) change dramatically with bombarding energy in the range 43–178 MeV in a manner which is reproduced with remarkable precision by our evaporation cal-

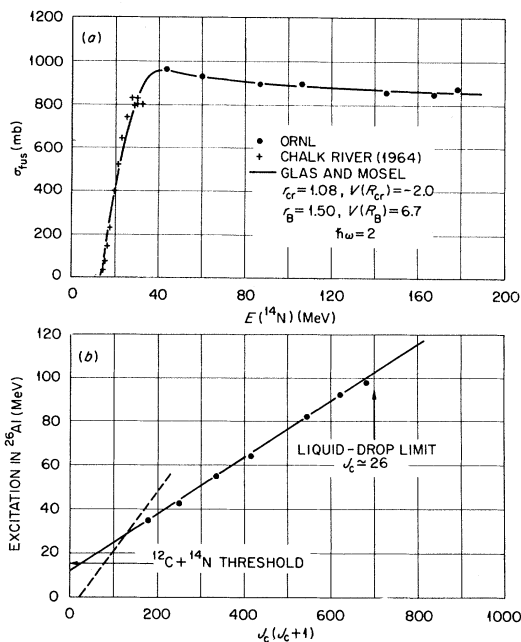


FIG. 2. (a) Measured fusion cross sections as a function of bombarding energy. The solid line is a theoretical fit to the data (see text). (b) Experimental values for the critical angular momenta versus excitation energy of the compound nucleus. The straight line defined by the measurements suggests a moment of inertia of  $2\mathcal{I}/\hbar^2 \sim 7.8 \text{ MeV}^{-1}$ . The expected position of the ground-state band is indicated by the dotted line.

ulation [see Fig. 1(b)]. It thus seems reasonable to conclude that processes analogous to deeply inelastic scattering do not contribute significantly to the yields which we identify as evaporation residues. However, one cannot rule out small contributions from such processes, particularly at the higher energies.

The experimental results are presented in Fig. 2(a) which also includes measurements by Kuehner and Almqvist<sup>8</sup> of  $\sigma_{\text{fus}}$  at lower energies. As the bombarding energy increases beyond 43 MeV up to 178 MeV, the value of  $\sigma_{\text{fus}}$  decreases gradually<sup>9</sup> from  $\sim 970 \text{ mb}$  to  $\sim 850 \text{ mb}$ . The rate of decrease is approximately proportional to  $1/E_{\text{c.m.}}$ . Under the assumption that fusion occurs when the nuclei penetrate to a critical radius,  $R_{\text{cr}} \equiv r_{\text{cr}}(A_1^{1/3} + A_2^{1/3})$ , it is possible to relate<sup>10</sup> the magnitude of the Coulomb-plus-nuclear potential  $V$  at  $R_{\text{cr}}$  to the magnitude and slope of  $\sigma_{\text{fus}}(E)$ . We use the model of Glas and Mosel<sup>10</sup> to fit the experimental data and deduce the parameters  $r_{\text{cr}} = 1.08 \text{ fm}$ ,  $V(R_{\text{cr}}) = -2 \text{ MeV}$ ,  $r_B = 1.5 \text{ fm}$ ,  $V(R_B) = 6.7 \text{ MeV}$  (the interaction barrier), and  $\hbar\omega = 2 \text{ MeV}$  [see Fig. 2(a)]. An interesting result is the shallow

nuclear potential,  $V_{\text{nuc}} \sim -14 \text{ MeV}$ , implied by the slow rate of decrease of  $\sigma_{\text{fus}}(E)$ . Shallow Woods-Saxon potentials have been used to fit elastic-scattering data for similar masses.<sup>11</sup> However, the derivatives  $|\partial V/\partial r|$  evaluated at  $R_{\text{cr}}$  are sufficiently small that the net radial force is repulsive at the point at which the nuclei are assumed to fuse. Furthermore, for partial waves with  $l \gtrsim 16$ , the radial force is repulsive at all points between  $R_{\text{cr}}$  and the interaction radius  $R_B$ . A folding model<sup>12</sup> can also account for the elastic scattering and predicts a nuclear force at  $R_{\text{cr}}$  sufficiently attractive to counter Coulomb and centrifugal repulsion. In this case, however, the value of  $V(R_{\text{cr}})$  is too negative to be consistent with the potential as deduced<sup>10</sup> from the measured slope of  $\sigma_{\text{fus}}$ . The Bass model,<sup>13</sup> which differs from that of Ref. 10 mainly in that it fixes  $R_{\text{cr}}$  at the half-density radius ( $r_{\text{cr}} = 1.0 \text{ fm}$ ) and uses a liquid drop model to determine the nuclear potential at  $R_{\text{cr}}$ , overestimates  $\sigma_{\text{fus}}$  for energies in the range 40–130 MeV but is in agreement for energies above 150 MeV.<sup>14</sup>

The above discussion of the fusion reaction in terms of simple one-dimensional potential models represents, of course, an idealization. We may expect that an understanding of the measured variation of  $\sigma_{\text{fus}}$  with energy will require a dynamical and multidimensional treatment of the interaction.<sup>2, 3</sup>

An alternative explanation is that  $\sigma_{\text{fus}}$  may be limited by the maximum angular momentum of the compound nucleus  $^{26}\text{Al}$  for a given excitation energy (i.e., the location of the yrast line). In Fig. 2(b) the experimental values of  $J_c(J_c + 1)$  defined by  $\sigma_{\text{fus}} = \pi\lambda^2(J_c + 1)^2$  are plotted versus excitation energy in  $^{26}\text{Al}$ . The data in Fig. 2(b) determine a straight line on a  $J_c(J_c + 1)$  scale which, for rigid rotation, indicates a moment of inertia  $2\mathcal{I}/\hbar^2 = 7.8 \text{ MeV}^{-1}$  and a band-head excitation energy of  $\sim 12 \text{ MeV}$ . The above moment of inertia corresponds, for example, to a  $^{26}\text{Al}$  nucleus undergoing rigid rotation with a deformation parameter  $\beta \simeq 0.4\text{--}0.5$ . This moment of inertia lies between the value corresponding to rigid rotation of a spherical ground state and the larger values calculated for a rotating deformable liquid drop.<sup>5</sup> (We note that the value of the inertial term  $2\mu R_{\text{cr}}^2/\hbar^2$  appearing in the centrifugal potential<sup>10</sup> in the entrance channel is also  $\sim 8 \text{ MeV}^{-1}$ .) The band head is located near the separation energy for  $^{26}\text{Al} \rightarrow ^{14}\text{N} + ^{12}\text{C}$ . Thus, the observed values of  $\sigma_{\text{fus}}$  at energies greater than 43 MeV may be explained by postulating a compound nucleus whose yrast

line is given by  $E_x = (7.8 \text{ MeV}^{-1})^{-1} J_c(J_c + 1) + 12 \text{ MeV}$ . Assuming only that an equilibrated compound nucleus is formed in this reaction, the yrast line must lie at or below that indicated by the straight line in Fig. 2(b). The experimental data therefore suggest that the  $^{26}\text{Al}$  nucleus (a) is deformed and undergoing rigid rotation for excitation energies  $E_x$  and angular momenta  $J_c$  given by the solid line in Fig. 2(b) and (b) has been formed at the highest bombarding energy with an angular momentum  $[(25.6 \pm 1.4)\hbar]$  equal to the limit for a rotating liquid drop,<sup>5</sup>  $\sim 26\hbar$ .

We are pleased to acknowledge the assistance of Dr. Roland Dayras in the measurements and discussions with Dr. F. Plasil, Dr. G. R. Satchler, and Dr. R. Y. Cusson.

\*Research supported by the U. S. Energy Research and Development Administration under contract with the Union Carbide Corporation.

†On sabbatical leave from Instituto de Física, Universidad Autónoma Nacional de México, México 20 D. F., México.

<sup>1</sup>B. Tamain, C. Ngô, J. Peter, and F. Hanappe, Nucl. Phys. **A252**, 187 (1975), and references therein.

<sup>2</sup>D. Glas and U. Mosel, Phys. Lett. **49B**, 301 (1974).

<sup>3</sup>P. Bonche, S. E. Koonin, and J. W. Negele, Phys. Rev. C **13**, 1226 (1976); R. Y. Cusson, R. K. Smith,

and J. A. Maruhn, Phys. Rev. Lett. **36**, 1166 (1976).

<sup>4</sup>J. Gomez del Campo, computer code LILITA (unpublished).

<sup>5</sup>S. Cohen, F. Plasil, and W. J. Swiatecki, Ann. Phys. (N.Y.) **82**, 557 (1974).

<sup>6</sup>R. G. Stokstad, in *Proceedings of the International Conference on Reactions Between Complex Nuclei, Nashville, Tennessee, 1974*, edited by R. L. Robinson, F. K. McGowan, J. B. Ball, and J. H. Hamilton (North-Holland, Amsterdam, 1974), Vol. II, p. 327, and references therein; C. Volant, M. Conjeaud, S. Harar, A. Lepine, E. F. DeSilveira, and S. M. Lee, Nucl. Phys. **A238**, 120 (1975); H. V. Klapdor, H. Reiss, and G. Rosner, Phys. Lett. **58B**, 279 (1975).

<sup>7</sup>R. Albrecht, W. Dünnweber, G. Graw, H. Ho, S. G. Steadman, and J. P. Wurm, Phys. Rev. Lett. **34**, 1400 (1975), and references therein.

<sup>8</sup>J. A. Kuehner and E. Almqvist, Phys. Rev. **134B**, 1229 (1964).

<sup>9</sup>The present results do not rule out the possibility of small oscillations in  $\sigma_{\text{fus}}$  such as have been observed for  $^{12}\text{C} + ^{16}\text{O}$  (ref. 8), and by P. Sperr, S. Vigdor, Y. Eisen, W. Henning, D. G. Kovar, T. R. Ophel, and B. Zeidman, Phys. Rev. Lett. **36**, 405 (1976).

<sup>10</sup>D. Glas and U. Mosel, Nucl. Phys. **A237**, 429 (1974). [Equation (12) was used to calculate  $\sigma_{\text{fus}}$ .]

<sup>11</sup>W. Reilly, R. Wieland, A. Gobbi, M. W. Sachs, and D. A. Bromley, Nuovo Cimento **13**, 897 (1973).

<sup>12</sup>G. R. Satchler, private communication.

<sup>13</sup>R. Bass, Phys. Lett. **47B**, 139 (1973).

<sup>14</sup>Results obtained recently for the fusion of  $^{12}\text{C} + ^{12}\text{C}$  at high energies by M. N. Namboodiri *et al.* (to be published) are consistent with the Bass model.

## Physical Basis for Enhanced Forward Cross Sections in Heavy-Ion Reactions\*

Norman K. Glendenning and Georg Wolschin†

Lawrence Berkeley Laboratory, University of California, Berkeley, California 94720

(Received 17 November 1975)

Calculations show that indirect transitions can explain the forward cross section observed in some experiments, in particular  $^{60}\text{Ni}(^{18}\text{O}, ^{16}\text{O})$ . Normal optical potentials which fit elastic and inelastic data are used in the analysis. An earlier analysis in terms of a surface transparent potential is shown to depend sensitively on a scaling factor that was introduced to simulate recoil effects. However when recoil is properly taken into account it is found that the surface transparent potential does not reproduce the data.

At moderate energies above the Coulomb barrier, quasi-elastic heavy-ion reactions are expected to exhibit a "grazing" peak in the differential cross section.<sup>1</sup> Brookhaven National Laboratory (BNL) experiments<sup>2</sup> produced the surprising result that several reactions of the type

$$^{60}\text{Ni}(^{18}\text{O}, ^{16}\text{O})^{62}\text{Ni}, \quad E = 65 \text{ MeV}, \quad (1)$$

had a large cross section forward of the grazing angle. Although indirect transfer can produce

such effects,<sup>3</sup> this was not at first suspected to be the explanation because the experiment did not reveal any likely candidates as intermediate states. The BNL group proposed a surface transparent optical potential with the property that the edge of the absorptive part is very sharp and lies inside the real part.<sup>4</sup> These authors employed a scaling factor in the relationship between the coordinates in their distorted-wave Born approximation (DWBA) calculation which is different